Image Clarification Method Based on Structure-Texture Decomposition with Texture Refinement

Masato Toda(✉), Kenta Senzaki, and Masato Tsukada

NEC Corporation, 1753 Shimonimabe, Kawasaki 211-8666, Japan
m-toda@ap.jp.nec.com, k-senzaki@bp.jp.nec.com,
m-tsukada@cj.jp.nec.com

Abstract. This paper presents a high quality and low complexity image clarification method, which restores the visibility of images captured in bad weather and poor lighting conditions. A sequential processing of conventional dehazing and backlit correction methods has a problem that textures and noises are over-emphasized by the corrections. The proposed method first decomposes a captured image into two components: a structure component forming smooth regions and strong edges and a rest component for fine textures and noises. Image enhancement is conducted based on analyses of the first component, while controlling an amplification factor of the texture component. The utilization of the structure component for the enhancement enables pixel-wise corrections without local area analysis which results in lower computational cost. Experimental results demonstrate that the proposed method can successfully enhance image qualities and its computational cost is reasonable for real-time video processing.

Keywords: Video surveillance · Image clarification · Image dehazing · Backlit correction

1 Introduction

Recently, video surveillance for outdoor purpose has attracted attention due to the fear of terrorism and violent criminals. In a surveillance system, operators catch occurrences of crimes or suspicious behaviors from the captured images. The performance of the system depends on the visibility of the images. To achieve a high security surveillance system and comfortable operations, captured images are required to be of high quality.

Image degradations in outdoor scenes are mainly caused by two kinds of environmental conditions. There are lighting conditions and weather conditions. The lighting condition affects brightness and the weather condition affects contrast of objects in an image (figure 1). Since it is difficult to control these environmental conditions physically, image restoration techniques are required.

Many methods have been proposed to enhance the image quality in poor lighting conditions, which modifies the dynamic range of the captured image virtually and provides high visibility [5, 10, 17, 19, 20]. These methods change tone-mapping curves for each pixel according to local area analysis. The image restoration in poor

V. Murino and E. Puppo (Eds.): ICIAP 2015, Part II, LNCS 9280, pp. 352–362, 2015.
DOI: 10.1007/978-3-319-23234-8_33

(a) Night scene (b) Backlit scene (c) Rainy scene (d) Dense foggy scene

Fig. 1. Images in bad environmental conditions.

lighting conditions is an established technique, it is widely used in many applications such as consumer digital cameras and imaging software.

The restoration of images in bad weather conditions is called "haze removal" or "image dehazing" and has been studied actively [2-4, 6-9, 11, 12, 16, 18]. Narashiman and Nayer proposed a physics-based scattering model, which can represent the light path in bad weather conditions, and showed that the scene structure can be recovered by captured images in different weather conditions [11, 12]. Schechner *et al.* proposed a dehazing method from two or more images with different polarized angles [16]. Single image dehazing is a more challenging problem, since there is fewer information available to estimate the haze-free scene. However, significant advances have been seen in recent years [2-4, 7-9, 18]. These advances are achieved based on the physics-based model with new prior about the scene. Tan proposed a method which restores the image by maximizing its local contrast [18]. Fattal proposed a retrieval method by using the relationship between the surface shading and the scene transmission that these are locally uncorrelated [2]. He *et al.* found that most local patches in haze-free images contain a pixel which has low intensity in at least one color channel and based on the prior, which is called dark channel prior, they recover vivid color images [3]. Refined methods based on the dark channel prior have been proposed [4, 8], because the dark channel prior is a simple but a effective prior. Since single image dehazing is conducted based on assumptions about the imaging model and the prior, it is quite possible that the image retrieval fails in some regions. As a result, the restored image tends to be dark and over-saturated [7].

Li *et al.* [7] proposed a post enhancement method after a single image dehazing to recover the degradation in the restored image using local area luminance. Their post enhancement is conducted with the similar concept to the enhancement in poor lighting conditions. Their work suggests that it is possible to achieve an image restoration in poor lighting and bad weather conditions, when a processing is executed in the order of a bad weather correction to a lighting correction, the lighting correction recovers the failure of the bad weather correction.

There are several problems still remain when the conventional methods are simply proceeded sequentially. One of the problems is the overemphasized textures by the correction. Since these corrections work as contrast enhancement, textures in captured images are emphasized by the corrections. The poor lighting correction recovers the failure in the bad weather correction in luminance level, however, it conducts an unnecessary enhancement in terms of textures. As a result, the corrected images become too sharp at these regions. The presence of noise in captured images is also an issue in

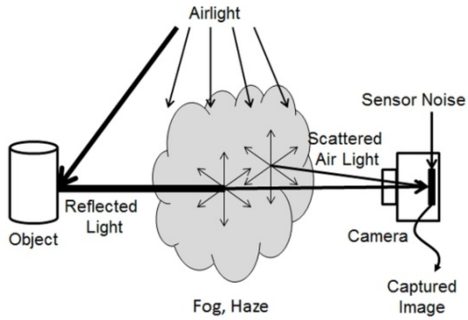

Fig. 2. Imaging model.

the corrected images. The noise is also emphasized by the corrections, and sometimes the noise becomes significantly visible by the enhancement even if it is hard to see in the original image. In addition, the computational cost becomes a problem, considering the case of implementation for image applications, because at least two local analyses are needed for the restoration.

To overcome these problems, this paper presents a new image clarification method based on structure-texture decomposition. The proposed method first decomposes a captured image into two components: a structure component forming smooth regions and strong edges and a rest component for fine textures and noises. A correction for bad weather and poor light is conducted based on analyses the structure component, while suppressing overemphasis in texture component. The utilization of the structure component for the enhancement enables pixel-wise corrections without local analyses which results in lower computational cost.

2 Imaging Model

In this section, the imaging model is presented. Figure 2 illustrates the path of lights which reach to an image sensor. In this model, an object is irradiated with airlight, and a reflected light is produced. The reflected light is attenuated by particles in the air before reaching the image sensor. The image sensor also captures airlight scattered by the particles. Finally the image sensor creates a captured image from these mixed lights with additive sensor noise.

It is well known that radiance of reflected light is related to irradiance of light and surface reflectance characteristics of object such as shape and albedo [13.14]. The radiance J is represented as equation (1), where x, c, l, A and R denote pixel position, color channel, irradiance of the incoming light, color composition of the airlight and the surface reflectance characteristics, respectively.

$$J^c(x) = l(x)\, A^c\, R^c(x) \tag{1}$$

The physics-based scattering model by Narasimhan and Nayer [11] is employed to represent the behavior of light passing through the air. Their model is simplified as equation (2) [2,3], where H denotes the intensity of mixed light irradiating the image sensor, t denotes the transmission for the scattering.

$$H^c(x) = t(x)J^c(x) + (1 - t(x))\, A^c \tag{2}$$

Assuming that the additive sensor noise is white gaussian noise with a variance σ, the intensity in captured image I is represented as equation (3), where η represents an intensity of the noise.

$$I^c(x) = \big(t(x)l^c(x)\, R^c(x) + (1 - t(x))\big)A^c + \eta^c(x) \tag{3}$$

In this imaging model, the change in lighting conditions is represented by l, and the change in weather conditions is represented by t. The degradation by image sensor noise and the effect by the color of the airlight are represented by η and A, respectively. Our target is to restore the captured image into an image in a good lighting and a fine weather condition represented as equation (4), where l_{ideal} denotes irradiance in a good lighting condition.

$$I_{ideal}^c(x) = l_{ideal}^c(x)\, R^c(x) \tag{4}$$

3 Proposed Method

3.1 Structure-Texture Decomposition

The proposed method first decomposes a captured image into two components: a structure component forming smooth regions and strong edges and a rest component for fine textures and noises. In general, irradiance and transmission change smoothly in an object and the significant changes occur at the boundaries of objects, which correspond to image edges. Therefore, an extraction of smooth regions preserving strong edges is useful for the analyses of these variables.

In this paper, total variation (TV) norm minimization [15] is employed for the decomposition, which can extract geometric features such as flat areas, monotonic changes, and steps in an input image, while separating oscillating signals such as fine textures, specular reflection light and noises. The processed image after the TV norm minimization is configured as the structure component and the residual is regarded as texture component in this paper. Processed images are shown in figure 3, where the texture component is amplified to five times.

The structure component and the texture component are approximately represented as equation (5) and (6), respectively, where R_s represents the body color of an object and R_t represents its textures. Since the noises are separated into the texture component, we can conduct noise-free analyses using the structure component.

$$S^c(x) = \big(t(x)\, l^c(x)\, R_s^c(x) + (1 - t(x))\big)A^c \tag{5}$$

$$T^c(x) = t(x)\, l^c(x)\, R_s^c(x)A^c + \eta^c(x) \tag{6}$$

(a) Input Image (b) Structure component (c) Texture component

Fig. 3. Structure-texture decomposition.

The structure-texture decomposition enables to predict the occurrence of overemphasized textures after corrections by observing the change in the texture component. The structure component contains much information about a surrounding region for each pixel. Therefore, utilization of the structure component enables pixel-wise corrections without local analysis which takes computational costs, just by sharing the change in the structure component during processing.

3.2 Airlight Correction

The effect by the airlight is removed as preprocessing in this paper. This processing is a kind of an automatic white balance correction. The airlight A is estimated by taking the top 1% brightest pixel for each color channel from the structure component where little specular reflection light is included. The captured image, the structure component and the texture component are corrected as equation (7).

$$I_1^c(x) = \frac{I^c(x)}{A^c}\ ,\ S_1^c(x) = \frac{S^c(x)}{A^c}\ ,\ T_1^c(x) = \frac{T^c(x)}{A^c} \tag{7}$$

The variance of the image sensor noise in the corrected image is also emphasized by the correction as equation (8).

$$\sigma_1^c = \sigma^c / A^c \tag{8}$$

3.3 Bad Weather Correction

An image dehazing is proceeded with a non-linear function based on the structure component in the proposed method. To conduct the image dehazing, the transmission t should be estimated for each pixel. In this paper, the transmission t is calculated as equation (9), which means strength of scatting in the air in an image is represented by a sum of a uniform coefficient α and regionally changing coefficient β.

$$t(x) = 1 - \big(\alpha + \beta(x)\big) \tag{9}$$

Since the dark channel prior is satisfied enough when it is applied to whole region in an image, α can be detected by equation (10) with high accuracy.

$$\alpha = \min_{\forall c}(\min_{\forall x}(I_1^c(x))) \tag{10}$$

β is estimated as equation (11) under an assumption that a residual of a dark channel in the structure component include the airlight with constant ratio k.

$$\beta(x) = k \cdot \min_{\forall c}(S_1^c(x) - \alpha) \tag{11}$$

The proposed method reduces the degradation by α and β separately. Since α can be detected with high accuracy as already mentioned, the restoration based on the physics-based scattering model works well. So proposed firstly remove the effect by coefficient α as equation (12) and creates a processed image I_2.

$$I_2^c(x) = \frac{1}{1-\alpha}(I_1^c(x) - \alpha) \tag{12}$$

The accuracy of the estimate value β is relatively lower than α, and the value of β includes a prediction error which causes dark and color over-saturated regions in a restored image. The degradation tends to be significant when it is applied to dark regions, because the correction amount by the scattering model increases while the region becomes dark. To avoid the problem, the proposed method conduct a restoration to reduce the effect by errors in β using a refined non-linear function represented in equation (13), and create a haze-free image I_3.

$$I_3^c(x) = (I_2^c(x))^{1/(1-\beta(x))} \tag{13}$$

This function has a characteristic that when it is applied to bright areas it works similar to the restoration using the physics-based scattering model like equation (12), and when it is applied to dark areas it reduces the correction amount not to make the area too dark. The proposed method conduct a restoration of structure component by the same procedure and create a haze-free structure component S_3.

3.4 Poor Lighting Correction

The haze-free structure component S_3 represents a brightness of a surrounding region at an interest pixel after the bad weather correction, including the effect by the failure of the bad weather correction. Thus, a poor lighting correction is conducted using the component S_3. The irradiance is estimated by taking the maximum value of each color channel in S_3 as equation (14). A scaling factor γ for the correction is calculated as equation (15), with the similar concept to a method in [20]. In equation (15), as the estimated irradiance l_{est} decreases, the scaling factor γ increases according to parameters a and b.

$$l_{est}(x) = \max_{\forall c}(S_3^c(x)) \tag{14}$$

$$\gamma(x) = max(-a\, l_{est}(x) + b, 1) \tag{15}$$

A corrected image I_4 is created as equation (16), while ensuring that the corrected image does not cause saturation.

$$I_4^c(x) = 1 - \left(1 - I_3^c(x)\right)^{\gamma(x)} \tag{16}$$

The proposed method also conducts a restoration of structure component by using the same way and create a processed structure component S_4.

3.5 Texture Refinement

Finally, the proposed method refines textures of the processed image after the poor lighting correction. The change in the texture component by the bad weather and the poor lighting correction is represented as equation (17).

$$r_c(x) = (I_4^c(x) - S_4^c(x))/T_1^c(x) \tag{17}$$

In order to suppress the excessive amplification of the texture component, the proposed method sets an upper limit value of the amplification factor r_{max} and modifies the texture component as equation (18) and (19).

$$T_2^c(x) = p(x)\, r^c(x)\, T_1^c(x) \tag{18}$$

$$p(x) = \begin{cases} r_{max} / \max_{\forall c}(r^c(x)) & if\ \max_{\forall c}(r^c(x)) > r_{max} \\ 1 & otherwise \end{cases} \tag{19}$$

Since the noise variance in the refined texture component T_2 can be estimated as equation (20), the proposed method conducts a soft threshold shrinkage for the noise reduction as equation (21).

$$\sigma_2^c(x) = p(x)\, r^c(x)\, \sigma_1^c \tag{20}$$

$$T_3^c(x) = \begin{cases} \mathrm{sgn}(T_2^c(x)) \cdot (|T_2^c(x)| > \sigma_2^c(x)) & if\ |T_2^c(x)| > \sigma_2^c(x) \\ 0 & otherwise \end{cases} \tag{21}$$

Finally, an output image I_{out} is created by combining the corrected structure component S_4 and the refined texture component T_3.

$$I_{out}^c(x) = S_4^c(x) + T_3^c(x) \tag{22}$$

4 Evaluation

Evaluations of the proposed method were` conducted using captured images in bad environmental conditions. Table 1 shows the parameter sets used for the evaluations. The same parameters are used for the restorations except for the noise variance in a night scene. In this paper, digital TV filter [1] is employed for the structure-texture decomposition, which can efficiently minimize the TV norm.

Table 1. Parameter sets for the evaluation.

Parameter	Value	Parameter	Value
Noise variance σ	0.005	Bad lighting correction parameter a	5.0
Noise variance σ (night scenes)	0.015	Bad lighting correction parameter b	4.0
Bad weather correction parameter k	0.85	Texture refinement parameter r_{max}	3.0

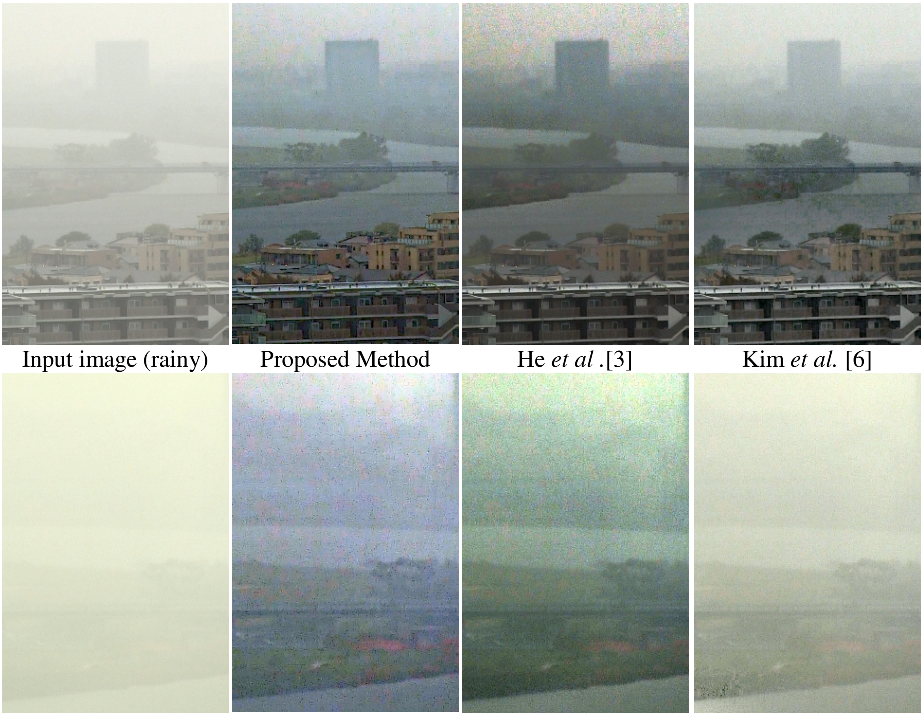

Input image (rainy) Proposed Method He *et al* .[3] Kim *et al.* [6]

Input image (foggy) Proposed Method He *et al.* [3] Kim *et al.* [6]

Fig. 4. Corrected images in bad weather conditions.

Figure 4 shows restored images in different bad weather conditions by the proposed method. The results by He *et al.* [3] and Kim *et al.* [6] are also shown in figure 4 for a comparison. The corrected images by He *et al.* [3] tends to be dark and color over-saturated as reported in [7] and noises in the captured image become significantly visible. The method by Kim *et al.* [6] does not cause dark or color over-saturated regions in the corrected images, however, the strength of the correction is very weak in the captured image in the foggy scene. On the other hand, our method successfully restores the image contrast failure in the bad weather condition, and create comfortable images, because our method recovers the failure in the bad weather correction while suppressing overemphasized textures and noises in the corrected images.

Fig. 5. Details of corrected images in bad weather conditions.

Fig. 6. Corrected images in bad weather conditions.

Figure 5 represents the differences of corrected images by the presence of the texture refinement procedure in the proposed method. The corrected images without the texture refinement indicate the corrected images when the conventional bad weather correction and the poor lighting correction are simply proceeded sequentially. In the corrected images without the texture refinement, the textures are overemphasized and become like a result of applying an unsharp mask which is not intended. The noises are also emphasized and become significantly visible. The proposed method adequately suppresses these overemphasized textures and noises.

Figure 6 demonstrates corrected images in poor lighting conditions by the proposed method. These results present that the proposed method also can successfully correct images in poor lighting conditions with the same parameters.

Table 2 shows the processing times of the proposed method to a VGA size image (640×480 pixels) on a CPU (Intel Xeon E5-1650 3.2GHz). The proposed method is

Table 2. Processing times of the proposed method.

Function	Processing time (ms)
Structure-texture decomposition	8.8
Airlight correction	2.0
Bad weather correction	5.0
Poor lighting correction	3.0
Texture refinement	1.5
Total	20.3

implemented using Intel AVX. The total time of the correction is 20.3 milliseconds. This result suggests that the proposed method can be embedded as software in actual imaging applications which require real-time video processing. The computational time is almost the same as the method by Kim *et al.* [6] (48.5 fps for VGA size video) which conducts only image dehazing. The notable point is that the computation of the bad weather and the poor lighting corrections takes less than 10 milliseconds. A sequential processing of the conventional dehazing and backlit correction methods requires filtering or optimization processes for local analyses which take relatively high computational costs in each correcting procedure. On the other hand, the enhancement based on the structure component in the proposed method enables pixel-wise corrections without any local analysis after the decomposition.

5 Conclusion

This paper has proposed a new image clarification method based on structure-texture decomposition, which can restore images captured in bad weather and poor lighting conditions. Image enhancement is conducted by an analysis of the structure component, while suppressing overemphasized textures and noises. Experiments demonstrated that the proposed method can successfully enhance image qualities and its computational cost is reasonable for real-time video processing.

Future studies include detailed subjective evaluation of the corrected images by the proposed method, in comparison with other conventional methods.

References

1. Chan, T.F., Osher, S., Shen, J.: The digial TV filter and nonlinear denoising. IEEE Transactions on Image Processing **10**(2), 231–241 (2001)
2. Fattal, R.: Single image dehazing. In: Proc. ACM SIGGRAPH 2008, pp. 1–9 (2008)
3. Huang, S.-C., Chen, B.-H., Wang, W.-J.: Visibility restoration of single hazy images captured in real-world weather conditions. IEEE Transactions on Circuits and Systems for Video Technology **24**(10), 1814–1824 (2014)

4. He, K., Sun, J., Tang, X.: Single image haze removal using dark channel prior. In: IEEE conference on Computer Vision and Pattern Recognition (CVPR) 2009, pp. 1956–1963 (2009)
5. Jobson, D.J., Rahman, Z.-U., Woodell, G.A.: A multiscale retinex for bridging the gap between color images and the human observation of scenes. IEEE Transactions on Image Processing **6**(7), 965–976 (1997)
6. Kim, J.-H, Jang, W.-D., Park, Y., Lee, D.-H., Sim, J.-Y., Kim, C.-S.: Temporally x real-time video dehazing. In: 19th IEEE International Conference on Image Processing, ICIP 2012, pp. 969–972 (2012)
7. Long, J., Shi, Z., Tang, W., Zhang, C.: Single remote sensing image dehazing. IEEE Geoscience and Remote Sensing Letters **11**(1), 59–63 (2014)
8. Li, B., Wang, S., Zheng, J., Zheng, L.: Single image haze removal using content-adaptive dark channel and post enhancement. IET Computer Vision **8**(2), 131–140 (2014)
9. Meng, G., Wang, Y., Duan, J., Xiang, S., Pan, C.: Efficient image dehazing with boundary constraint and contextual regularization. In: 2013 IEEE International Conference on Computer Vision (ICCV), pp. 617–624 (2013)
10. Monobe, Y., Yamashita, H., Kurosawa, T., Kotera, H.: High dynamic range compression for digital video camera using local contrast enhancement. In: International Conference on Consumer Electronics (ICCE) 2015, Digest of Technical Papers, pp. 217–218 (2005)
11. Narasimhan, S.G., Nayer, S.K.: Vision and the Atmosphere. International Journal on Computer Vision **48**(3), 233–254 (2002)
12. Narasimhan, S.G., Nayer, S.K.: Contrast Restoration of Weather Degraded Images. IEEE Transactions on Pattern Analysis and Machine Intelligence **25**(6), 713–724 (2003)
13. Oren, M., Nayer, S.K.: Generalization of lmbert's reflectance model. In: ACM SIGGRAPH 1994, pp. 239–246 (1994)
14. Phong, B.T.: Illumination for computer generated pictures. Commun. ACM **18**(6), 311–377 (1975)
15. Rudin, L.I., Osher, S., Fatemi, E.: Nonlinear total variation based noise removal algorithms. Physica D: Nonlinear Phenomena **60**(1–4), 259–268 (1992)
16. Shimoyama, S., Igarashi, M., Ikebe, M., Motohisa, J.: Local adaptive tone mapping with composite multiple gamma functions. In: 16th IEEE International Conference on Image Processing (ICIP 2009), pp. 3153–3156 (2009)
17. Schechner, Y.Y., Narasimhan, S.G., Nayer, S.K.: Polarization-Based Vision through Haze. Applied Optics, Special issue **42**(3), 511–525 (2009)
18. Tan, R.T.: Visibility in bad weather from a single image. In: IEEE Conference on Computer Vision and Pattern Recognition (CVPR) 2008, pp. 1–8 (2008)
19. Toda, M., Tsukada, M.: High dynamic range rendering method for YUV images with global luminance correction. In: IEEE International Conference on Consumer Electronics (ICCE) 2011, pp. 255–256 (2011)
20. Toda, M., Tsukada, M., Inoue, A., Suzuki, T.: High dynamic range rendering for YUV images with a constraint on perceptual chroma preservation. In: 16th IEEE International Conference on Image Processing (ICIP 2009), pp. 1817–1820 (2009)